= ATOMS, MOLECULES, OPTICS =

SOURCE OF ULTRACOLD ATOMS ⁸⁷RB FOR ATOMIC INTERFEROMETER-GRAVIMETER

© 2024 A. E. Bonert^a, A. N. Goncharov^{a,b,c}, D. N. Kapusta^{a,b,*}, O. N. Prudnikov^{a,b}, A. V. Taichenachev^{a,b}, and S. N. Bagaev^{a,b}

^aInstitute of Laser Physics Siberian Branch of the Russian Academy of Sciences, Novosibirsk, 630090 Russia ^bNovosibirsk State University 630090, Novosibirsk, Russia Novosibirsk State Technical University, Novosibirsk. 630073 Russia

*e-mail: dmitriikapusta@mail.ru

Received March 12, 2024 Revised May 06, 2024 Accepted May 06, 2024

Abstract. The results of experimental studies on creating a source of ultracold atoms ⁸⁷Rb for an absolute quantum gravimeter based on atomic interference are presented. The studies resulted in sub-Doppler cooling of atoms ⁸⁷Rb in a magneto-optical trap and in obtaining a cloud $\sim 10^7 - 10^8$ of atoms with a temperature of 6 MKK. Using microwave radiation and optical pumping, the preparation of ultracold atoms in the initial state $|F=1,m_F=0\rangle$ is carried out and experiments are performed to observe Ramsey resonances at the transition $|F=1,m_F=0\rangle \rightarrow |F=2,m_F=0\rangle$ during the interaction of the atomic cloud with unidirectional Raman radiation pulses.

The article is presented as part of the conference proceedings "Physics of Ultracold Atoms" (PUCA-2023), Novosibirsk, December 2023.

DOI: 10.31857/S004445102410e02X

1. INTRODUCTION

Creating high-precision sensors is one of the key challenges in precision measurements. The development of ultra-sensitive quantum sensors based on ultracold atom interference opens up great prospects for creating a new generation of instruments and devices such as accelerometers, gravimeters, gravitational field gradiometers, gyroscopes combining high metrological characteristics with compactness and mobility [1-3]. Much attention is paid to the development of absolute quantum gravimeters based on ultracold atoms that demonstrate record-high sensitivity, long-term stability, and measurement accuracy as compared to other types of sensors [4, 5] and are of great interest to fundamental metrology (mass standard, frequency standards), navigation, geophysics, etc. [6]. The decisive factor in achieving such characteristics is the quality of the ultracold atom source underlying the atomic gravimeter. In

particular, serious requirements are imposed on such source parameters as the number of cold atoms, their temperature and phase density, the efficiency of initial wave packet preparation, reproducibility of these parameters from cycle to cycle, etc.

This work was aimed at creating a source of ultracold atoms ⁸⁷Rb for an absolute quantum gravimeter based on atomic interference.

2. EXPERIMENTAL SETUP

This section presents a detailed description of the experimental setup (Fig. 1) developed by us to implement efficient laser cooling and trapping of rubidium atoms in a classical magneto-optical trap (MOT) [7].

The optical ptical scheme of the ultracold atom source ⁸⁷Rb is shown in Figs. 2*a*, *b*. The optical trap system (Fig. 2*a*) was implemented based on the Toptica DLpro laser system providing maximum

BONERT et al.

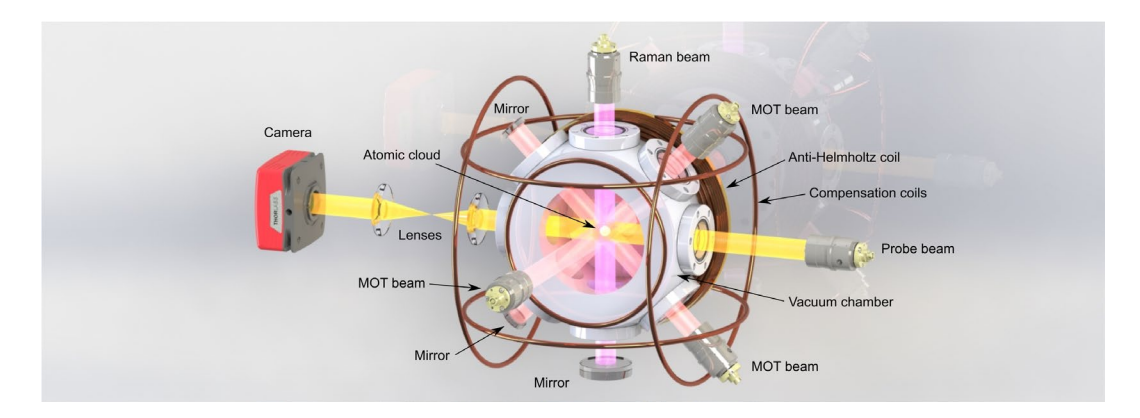


Fig. 1. Three-dimensional model of the experimental setup used in this work. The figure shows the vacuum chamber, three pairs of compensation magnetic coils, cooling laser beams (pink), Raman beams (purple), probe beam (yellow), optics (collimators, mirrors, lenses), and video camera. The quarter-wave plates and anti-Helmholtz coil (front side) are not shown in the figure

output radiation power of over 1 W at a wave of \sim 780.24 nm. The laser system frequency was stabilized using saturated absorption resonances on the $|F = 2\rangle \rightarrow |F' = 3\rangle$ transition in the ⁸⁷Rb atom. To form cooling laser beams, part of the radiation at the output of the tapered amplifier (TA, see Fig. 2a) was passed through two sequential acoustooptic modulators (AOM) to create a frequency detuning towards the long-wavelength region of the optical spectrum relative to the transition frequency $|F=2\rangle \rightarrow |F'=3\rangle$. This detuning was optimized, with its value being 13 MHz. The formation of "repumping" radiation with a frequency equaling the transition frequency $|F=1\rangle \rightarrow |F'=2\rangle$, was achieved using a fiber phase electro-optic modulator (EOM) with a microwave frequency of 6.654 GHz.

The positive first-order sideband was used. Other components in the radiation spectrum at the EOM output did not have a noticeable parasitic effect on the cooling efficiency. The cooling and repumping radiation were combined using a fiber polarization beam combiner (Thorlabs PFC780A) and then divided into three equal parts. This radiation was delivered to the vacuum chamber using polarization-maintaining single-mode fibers and collimators providing an output beam diameter of about 1 cm (FWHM). The total output power of the cooling and repumping lasers for all three beams was approximately 40 and 2.5 mW, respectively. These beams, through their retroreflection, formed three mutually orthogonal pairs of laser beams with appropriate circular polarization required for laser cooling.

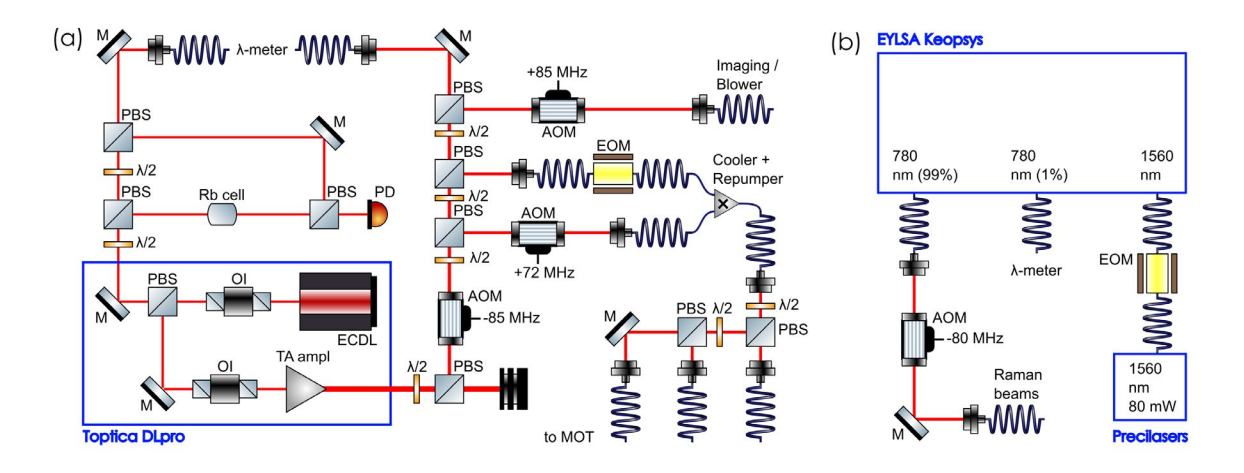


Fig. 2. Optical scheme for generating laser radiation used for laser cooling and trapping of rubidium atoms (a) and implementation of two-photon Raman transitions in atomic interferometer (b). Designations: AOM is the acousto-optic modulator, EOM is the electro-optic modulator, ECDL is the external cavity diode laser, λ / 2 is a half-wave plate, M is the mirror, OI is the Faraday optical isolator, PBS is the polarizing beam splitter, and TA ampl is the optical amplifier. Only the first diffraction order at the AOM output is shown

The quadrupole magnetic field was created by two coils in anti-Helmholtz configuration. The magnetic field gradient value at the center of the vacuum chamber was about 15 G/cm. To compensate for the residual magnetic field at the center of the vacuum chamber, three pairs of Helmholtz compensation coils were used, with their axes oriented along three mutually orthogonal directions.

The spatial distribution of the atomic cloud's optical density was registered using absorption and fluorescence methods. The optical scheme of the absorption registration method included a probe laser beam with its radiation frequency equaling the transition frequency $|F=2\rangle \rightarrow |F'=3\rangle$, and a power of < 1 mW, a lens system, and a CMOS video camera (Thorlabs 4070M-USB-TE). The atomic cloud fluorescence signal was formed as a result of atomic irradiation output by cooling laser beams and was registered using a CMOS video camera and photomultiplier tube (PMT). The temperature of the atomic cloud was determined by its expansion rate during free flight [8].

3. SUBDOPPLER COOLING OF RUBIDIUM ATOMS

In the magneto-optical trap, we obtained a cloud of $\sim 10^7-10^8$ cold atoms 87 Rb with a temperature of about 180 μ K, which is close to the Doppler limit. To cool atoms to lower temperatures, it is necessary

to use deep sub-Doppler cooling methods [8–10]. In this work, further cooling of rubidium atoms was performed by us in an "optical molasses". The effectiveness of this method depends on how much the light shift dominates over the Zeeman shift of the ground state sublevels in the atom. To achieve the lowest atomic temperatures in the "optical molasses", it is necessary to minimize the magnetic field value and its gradients in the cooling beams overlap region.

In this work, the magnetic fields were registered using microwave spectroscopy of magnetic dipole transitions between Zeeman sublevels of the states $|F=1,2\rangle$, whose frequency is proportional to the magnetic field. A directional microwave antenna, microwave generator, and microwave signal amplifiers were used to generate microwave radiation. Microwave radiation pulses were formed using a 16-channel synchronous timer and a switch (ZSWA4-63DR+). The polarization direction of microwave radiation was changed by rotating the antenna in a plane perpendicular to the radiation propagation direction.

A typical experimental cycle lasted about 150 ms and consisted of the following sequence: cooling and trapping atoms in MOT; pumping atoms to sublevels of the "dark" state $|F=1\rangle$ using only cooling beams without repumper; irradiating atoms with a microwave pulse at the frequency v_{MW} , causing

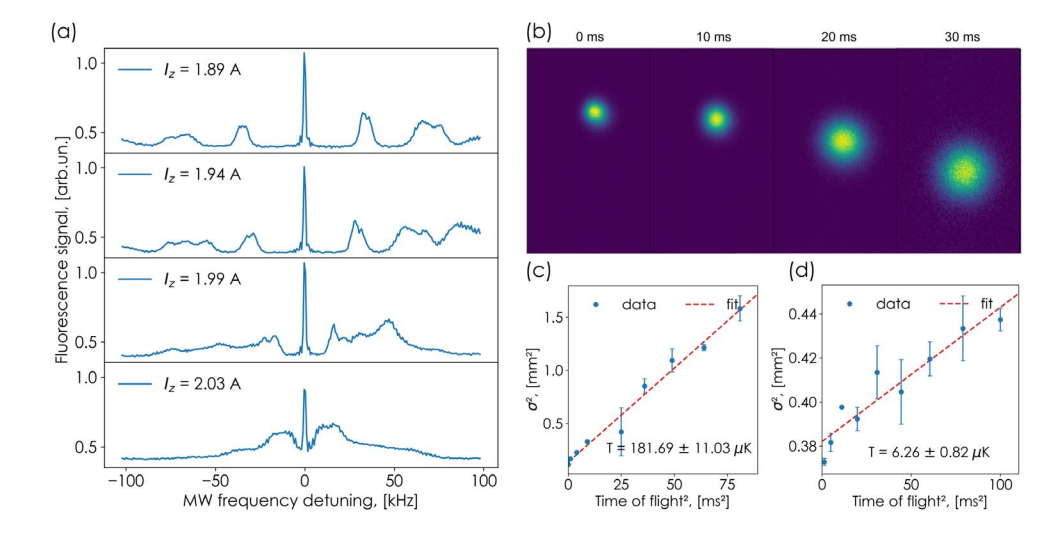


Fig. 3. Implementation of effective sub-Doppler cooling of rubidium atoms in "optical molasses": graphs showing atomic cloud fluorescence signal dependence on microwave radiation frequency detuning relative to the clock transition frequency in the atom ⁸⁷Rb at different currents in compensation coils generating magnetic field along the vector $\mathbf{g}(a)$; demonstration of temporal evolution of the atomic cloud size after cooling is completed in "optical molasses" (b); graphs showing dependence of the squared cold atom cloud size σ^2 on the squared free fall time for Doppler (c) and sub-Doppler (d) cooling

438 BONERT et al.

the atom to transition to one of the sublevels of the "bright" state $|F=2\rangle$; the final stage of registering atoms in the state $|F=2\rangle$ by re-enabling cooling beams without repumper.

Figure 3a shows a typical spectra of magnetic dipole transitions obtained by scanning the frequency v_{MW} near the hyperfine splitting frequency of the ground state in the rubidium atom. The value of the residual magnetic field B calculated from the following relation [11]: $B = \Delta v/(g_F \mu_B)$, where $g_F = 1/2$ is the Lande factor, $\mu_R = 1.4 \text{ MHz/G}$ is the Bohr magneton, Δv is the frequency difference between two adjacent magnetic dipole transitions for which $\Delta m_E = 1$, equaling the distance between two adjacent resonances shown in Fig. 3a. To compensate for the magnetic field, resonances of magnetic dipole transitions were recorded and the distance between them Δv was minimized by adjusting the currents in the compensation coils. The minimum achieved value of residual magnetic fields was about 10 mG.

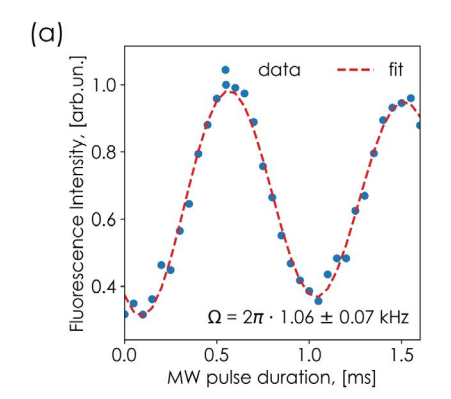
The stage of cooling atoms in the "optical molasses" began after switching off the quadrupole magnetic field, which had a decay time of about 5 ms, and lasted 10 ms. During this time, the detuning of the cooling laser radiation frequency changed from 13 to 50 MHz while its power decreased by a factor of 10. As a result of our implemented sub-Doppler cooling, we managed to lower the temperature of rubidium atoms to approximately 6 μ K and avoid significant atom losses at the end of the cooling stage in the "optical molasses". Figs. 3 c and d show graphs of the dependence of the σ^2 atomic cloud size squared on the free-fall time squared allowing us to

evaluate the effectiveness of sub-Doppler cooling as compared to the Doppler technique.

4. SELECTION OF ATOMS INTO NON-MAGNETIC STATE

The interaction of a magnetic field with a cloud of atoms in a state with non-zero magnetic moment is an additional source of decoherence in the atomic interferometer and reduces the contrast of the interference signal [12]. The solution to this problem is to prepare an ensemble of atoms in a non-magnetic quantum state, which serves as the initial wave packet in the atomic interferometer. In particular, in this work, the selection of atoms into the ground state $|F=1, m_F=0\rangle$ was performed using microwave and optical radiation. The main reason for choosing this method was its relative simplicity of implementation, which did not require an additional laser radiation source, which is necessary, for example, in optical pumping in a twofrequency linearly polarized laser field [13].

The atom selection was carried out according to the following scheme. By the end of the cooling stage, atoms distributed across Zeeman sublevels of ground states were pumped to sublevels of the state $|F=2\rangle$ using a repumper for 1.5 ms. Upon completion of the pumping process, the fraction of atoms in the state $|F=2,m_F=0\rangle$, was transferred to the state $|F=1,m_F=0\rangle$ by applying a π -pulse of microwave radiation with a frequency equaling the clock transition frequency in the rubidium atom. The final stage involved removing the remaining atoms in the state $|F=2\rangle$ from the detection zone



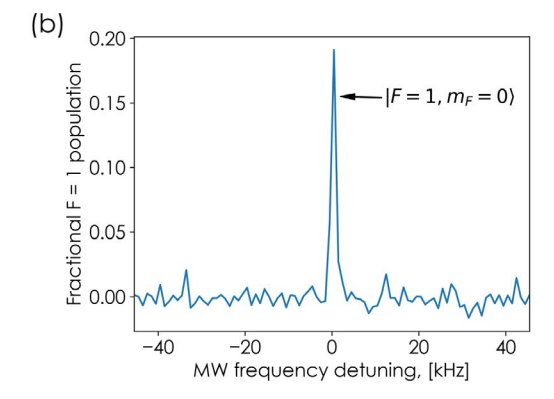
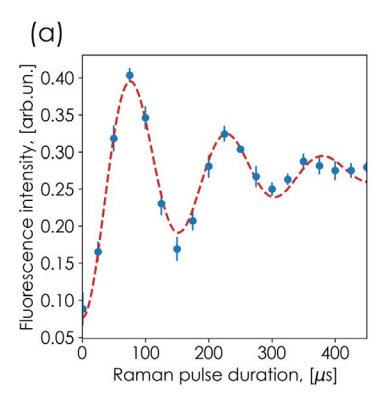
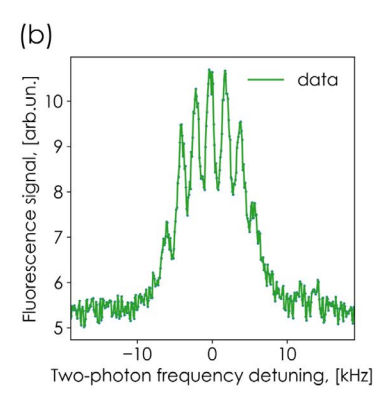


Fig. 4. Selection of atoms in a non-magnetic quantum state: Rabi oscillations graph recorded for the transition $|F=1,m_F=0\rangle \leftrightarrow |F=2,m_F=0\rangle$ by varying the duration of the microwave pulse (a); graph showing the population of atoms in the state $|F=1,m_F=0\rangle$ versus microwave radiation frequency detuning (b)





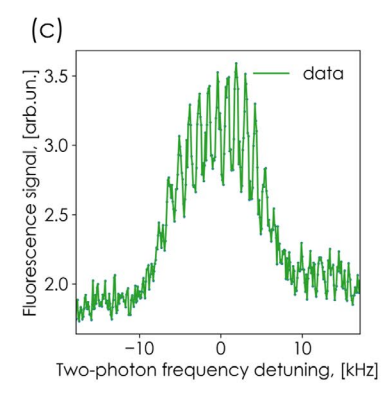


Fig. 5. Registration of Ramsey resonances: Rabi oscillations graph obtained for the two-photon transition $|F=1, m_F=0\rangle \leftrightarrow |F=2, m_F=0\rangle$ (a); Ramsey resonance diagrams recorded by scanning the frequency difference of two co-directed Raman beams, at times 600 µs (b) and 800 µs (c) between pulses

by "blowing" them away with resonant probe beam radiation. To split the magnetic sublevels, a uniform magnetic field of 200 mG was used, directed along the free-fall acceleration vector g and created by changing the current for the corresponding pair of compensation coils.

To implement effective atom selection. Rabi oscillations for the two-level transition $|F=1,m_F=0\rangle \leftrightarrow |F=2,m_F=0\rangle$ preliminarily recorded by varying the duration of the microwave radiation pulse (Fig. 4a). Under our experimental conditions, the duration of the π -pulse of the microwave signal was about 470 μ s. In our scheme, the maximum possible fraction of selective atoms from the initial total number of atoms equals %. Fig. 4b shows that at zero detuning of the microwave radiation frequency from the clock transition frequency in the atom ⁸⁷Rb, the fraction of atoms prepared in the state $|F=1, m_F=0\rangle$, was more than 15%. In the future, to increase the efficiency of atomic population in this nonmagnetic sublevel, we plan to use an alternative method of optical pumping by linearly polarized laser radiation, where the efficiency can reach 100%, as demonstrated, for example, in [13].

5. ATOMIC INTERFERENCE

To register atomic interference in this work, we developed and implemented an optical scheme for forming Raman beams. It is shown in Fig. 2b. The implementation of two-photon Raman transitions requires laser radiation generated at two frequencies ω_1 and ω_2 and detuned in frequency from the nearest allowed transition by several GHz. This detuning Δ

was formed relative to the excited transition $|F'=1\rangle$ and varied in the range of 0.5–2.5 GHz. The frequency difference $\Delta\omega=\omega_1-\omega_2$ was near the hyperfine splitting frequency of the ground state in the atom ⁸⁷Rb and could be detuned from it by $\delta\omega$.

In our optical scheme, the Raman beam radiation I_1 with the radiation frequency ω_1 was generated by a fiber laser system (Precilasers fiber laser with $\lambda = 1560$ nm and EYLSA Keopsys amplifier/frequency doubler). The beam radiation I_2 with the frequency ω_2 was formed using a phase EOM - a positive first-order band. The intensity ratio of Raman beams I_1/I_2 and detuning $\delta\omega$ were controlled by the power and frequency of the microwave generator, respectively. Raman radiation pulses were formed using AOM and delivered to the vacuum chamber through a polarizationmaintaining single-mode fiber and a collimator. The collimated radiation passed through the vacuum chamber and quarter-wave plate, reflected from the mirror, and formed a counter-propagating beam. The wave plate was adjusted to form a *lin*⊥*lin* polarization configuration of counter-propagating beams. In experiments aimed at suppressing Stark shifts and detecting Ramsey resonances, one pair of co-propagating Raman beams with σ^- -polarization was used. The propagation direction of Raman beams was set parallel to the g vector.

In the scheme with two Raman pulses and freely falling cloud of cold rubidium atoms, we observed the interference signal — Ramsey resonances [14, 15]. The duration of each $\pi/2$ -pulse was about 40 μ s (Fig. 4a). Figures 5b and 5c show images of two interference signals obtained for different times between pulses.

6. CONCLUSIONS

We created an ultracold atom source for a quantum interferometer-gravimeter based on MOT. A cloud of $\sim 10^7-10^8$ atoms ⁸⁷Rb with a temperature of about 6 μ K was obtained. Compensation of the residual magnetic field to the level of about 10 mG was performed using microwave spectroscopy of magnetic dipole transitions, which allowed for deep sub-Doppler cooling of atoms. Their selective microwave and optical pumping into the ground non-magnetic quantum state $|F=1,m_F=0\rangle$ was achieved in quantities exceeding 15% of the initial number of atoms in MOT. Two-photon Raman transitions between ground states $|F=1,2\rangle$ were studied and atomic interference, viz. Ramsey resonances, was registered.

In the future, we plan to implement an atomic interferometer using a three-pulse scheme with counter-propagating Raman beams and a spin free evolution time of more than 10 ms, and proceed directly to measuring the magnitude of the gravitational acceleration. To compensate for the additional frequency detuning arising from the Doppler shift caused by the free fall of atoms, we will implement a chirping technique for the frequency detuning of $\delta\omega$ Raman beams. To minimize the impact of optical element vibrations on the atomic interferometer signal, we plan to use passive vibration isolation system.

ACKNOWLEDGEMENTS

The authors express their gratitude to S. A. Farnosov and V. A. Vasiliev for their assistance in manufacturing and adjusting the electronic systems used in the research.

FUNDING

This work was supported by the Russian Science Foundation (grant No. 23-12-00182).

REFERENCES

- 1. R. Geiger, A. Landragin, S. Merlet et al., AVS Quantum Sci. 2, 024702 (2020).
- 2. G. M. Tino and M. A. Kasevich, *Atom Interferometry, Proc. Int. School of Physics «Enrico Fermi»*, Amsterdam (2014).
- 3. N. Heine, J. Matthias, M. Sahelgozin et al., Eur. Phys. J. D **74**, 174 (2020).
- **4**. S. Abend, M. Gebbe, M. Gersemann et al., Phys. Rev. Lett. **117**, 203003 (2016).
- 5. S. M. Dickerson, J. M. Hogan, A. Sugarbaker et al., Phys. Rev. Lett. **111**, 083001 (2013).
- **6**. K. Bongs, M. Holynski, J. Vovrosh et al., Nat. Rev. Phys. **1**, 731 (2019).
- 7. E. L. Raab, M. Prentiss, A. Cable, S. Chu et al., Phys. Rev. Lett. **59**, 2631 (1987).
- **8**. P. D. Lett, W. D. Phillips, S. L. Rolstone et al., J. Opt. Soc. Amer. B **6**, 2084 (1989).
- 9. J. Dalibard and C. Cohen-Tannoudji, J. Opt. Soc. Amer. B **6**, 2023 (1989).
- **10**. C. Salomon, J. Dalibard, W. D. Phillips et al., Europhys. Lett. **12**, 683 (1990).
- 11. D. A. Steck, URL: http://steck.us/alkalidata (2001).
- **12**. M. Kasevich and S. Chu, Appl. Phys. B **6**, 321 (1992).
- **13**. I. I. Beterov, E. A. Yakshina, D. B. Tretyakov et al., JETP **159**, 409 (2021).
- 14. N. F. Ramsey, Phys. Rev. 78, 695 (1950).
- **15**. Y. Feng, H. Xue, X. Wang et al., Appl. Phys. B **118**, 139 (2015).